GPR56 Promotes Diabetic Kidney Disease Through eNOS Regulation in Glomerular Endothelial Cells

Jinshan Wu,[1,2] Zhihong Wang,[1,3] Minchao Cai,[1] Xuan Wang,[1] Benjamin Lo,[1] Qifu Li,[3] John Cijiang He,[1,4] Kyung Lee,[1] and Jia Fu[1]

Diabetes 2023;72:1652–1663 | https://doi.org/10.2337/db23-0124

Although glomerular endothelial dysfunction is well recognized as contributing to the pathogenesis of diabetic kidney disease (DKD), the molecular pathways contributing to DKD pathogenesis in glomerular endothelial cells (GECs) are only partially understood. To uncover pathways that are differentially regulated in early DKD that may contribute to disease pathogenesis, we recently conducted a transcriptomic analysis of isolated GECs from diabetic *NOS3*-null mice. The analysis identified several potential mediators of early DKD pathogenesis, one of which encoded an adhesion G protein–coupled receptor-56 (GPR56), also known as ADGRG1. Enhanced glomerular expression of GPR56 was observed in human diabetic kidneys, which was negatively associated with kidney function. Using cultured mouse GECs, we observed that GPR56 expression was induced with exposure to advanced glycation end products, as well as in high-glucose conditions, and its overexpression resulted in decreased phosphorylation and expression of endothelial nitric oxide synthase (eNOS). This effect on eNOS by GPR56 was mediated by coupling of $G\alpha_{12/13}$–RhoA pathway activation and Gαi-mediated cAMP/PKA pathway inhibition. The loss of GPR56 in mice led to a significant reduction in diabetes-induced albuminuria and glomerular injury, which was associated with reduced oxidative stress and restoration of eNOS expression in GECs. These findings suggest that GPR56 promotes DKD progression mediated, in part, through enhancing glomerular endothelial injury and dysfunction.

ARTICLE HIGHLIGHTS

- Glomerular endothelial cell dysfunction is a key component of diabetic kidney disease (DKD) pathogenesis, but underlying molecular mechanisms are not entirely understood.
- Unbiased expression identified GPR56, a versatile adhesion G protein–coupled receptor, as a potential mediator of glomerular endothelial cell function in DKD, but its role in endothelial or kidney cells was not well understood.
- This study unravels the role of GPR56 in glomerular endothelial cells in DKD and demonstrates that it is a key mediator of DKD progression.
- The targeting of GPR56 may be a novel therapeutic approach in DKD.

Glomerular endothelial dysfunction has long been implicated in the pathophysiology of diabetic kidney disease (DKD) (1–3). Dysregulated expression of various endothelial factors (4), decreased nitric oxide availability (5–7), and disturbances in the endothelial barrier (8,9) are implicated in the disease pathogenesis. Moreover, endothelial dysfunction is noted in the early stages of disease progression, antecedent to the development of podocyte foot process effacement and microalbuminuria (10,11). To explore the molecular changes that occur in glomerular endothelial cells (GECs) in early DKD, we recently undertook a bulk transcriptomic analysis of isolated GECs from streptozotocin (STZ)-induced diabetic mice with endothelial nitric oxide synthase (eNOS) deficiency (12) and single-cell transcriptomic analysis of glomerular cells from

[1]Department of Medicine, Division of Nephrology, Icahn School of Medicine at Mount Sinai, New York, NY
[2]Department of Endocrinology, The First Affiliated Hospital of Chongqing Medical University, Chongqing, China
[3]Department of Endocrinology, The First Affiliated Hospital of Chongqing Medical University, Chongqing, China
[4]Renal Program, James J. Peters Veterans Affairs Medical Center at Bronx, Bronx, NY

Corresponding author: Kyung Lee, kim.lee@mssm.edu, or John Cijiang He, cijiang.he@mssm.edu, or Jia Fu, jia.fu@mssm.edu

Received 10 February 2023 and accepted 9 August 2023

This article contains supplementary material online at https://doi.org/10.2337/figshare.23926191.

J.W. and Z.W. contributed equally to this work.

the same mouse model (13). These studies identified several genes that were upregulated in GECs of diabetic mice, such as leucine-rich α-2-glycoprotein (*Lrg1*), whose roles in kidney disease had not been previously investigated. We subsequently demonstrated that increased LRG1 expression, indeed, promotes DKD through the endothelial activation via the potentiation of TGF-β/ALK1 signaling and that its loss attenuated the development of diabetic glomerulopathy (14). Another highly upregulated gene in GECs of diabetic mice that was identified in the previous study is adhesion G protein–coupled receptor (GPCR) G1 (encoded by *Adgrg1*), also known as G protein–coupled receptor 56 (GPR56) (12). GPR56 is a versatile adhesion GPCR whose functions are important for cell adhesion, neurobiological processes for the central and peripheral nervous systems, hematopoietic stem cell generation, muscle hypertrophy, immune regulation, hematopoietic stem cell generation, and tumorigenesis (15,16). As such, its aberrant expression or function is implicated in a variety of pathological processes, such as cancer malignancies, autoimmune and inflammatory diseases, and nervous system disorders. GPR56 is activated through various ligands, such as transglutaminase 2, extracellular matrix (ECM) molecules, and heparin sulfate (17–19), and elicits downstream signals via $G\alpha_{12/13}$-mediated activation of RhoA and Gi-mediated inhibition of cAMP/PKA (20,21). Like other adhesion GPCRs, GPR56 also functions as a sensor of shear stress (22). However, although GPR56 has been reported to regulate VEGF secretion and angiogenesis in melanoma (23), its role in the context of kidney disease has not been explored. Because high-glucose conditions can induce GPR56 expression in GECs (12) and shear stress is increased during glomerular hyperfiltration in diabetic kidneys, in the present study, we further investigated the role of GPR56 in GECs in vitro and the effects of its loss on DKD progression in vivo.

RESEARCH DESIGN AND METHODS

Mouse GEC Culture

Immortalized mouse GECs were cultivated as previously described (12). Lentiviral vectors expressing either scrambled shRNA (shScr) or GPR56 shRNA was purchased from Sigma-Aldrich (MISSION shRNA). The plasmid for overexpression of GPR56, pCAG-hGPR56-IRES-GFP, was purchased from Addgene (catalog no. 52297). KLF4 knockdown in endothelial cells was performed using the Genecopoeia lentiviral synthetic shRNA stems embedded into the context of endogenous miRNAs (shRNAmir) system with HSH022519–21-LVRU6GP (KLF4-shRNA21) and CSHCTR001-LVRU6GP (Scr-shRNA) constructs. Overexpression for KLF4 (LentiORF-KLF4) was purchased from Genecopoeia. Lentiviral particles were produced by cotransfecting HEK293T cells with, pCD/NL-BH*DDD packaging plasmid (Addgene; catalog no. 17531) and VSV-G–encoding pLTR–G plasmid (Addgene; catalog no. 17577). For lentiviral transduction, endothelial cells were incubated with viral supernatants for 24 h, followed by puromycin selection for an additional 72 h prior to use in all studies. Mouse GECs (mGECs) were incubated with 10 μmol/L H-89 dihydrochloride (ChemCruz; catalog no. SC-3537A), Fasudil (HA-1077; Selleckchem, catalog no. S1573), or vehicle (DMSO) for 24 h, as specified.

Quantitative RT-CR

Primers for RT-PCR were designed by using Primer-Blast (National Center for Biotechnology Information) (Supplementary Table 1). Gene expression was normalized to Gapdh, and fold change in expression relative to the control group was calculated using the comparative cycle threshold method. Two or more technical replicates per gene were used per experiment.

Mouse Model

Mice were housed in a specific pathogen-free facility with free access to chow and water and a 12-h day-to-night cycle. The *Adgrg1*^{tm1Lex}/Mmucd mouse strain on a mixed C57BL/6J and 129S5 background was obtained from the Mutant Mouse Resource and Research Center (catalog no. 032341-UCD), and genotyping was performed with the following primers: *1*) DNA085–5 (5′-CGA GAA GAC TTC CGC TTC TG-3′); 2) DNA085–14 (5′-AAA GTA GCT AAG ATG CTC TCC-3′); and *3*) Neo3a (5′-GCA GCG CTA CGCCTT CTA TC-3′). Because Gpr56$^{-/-}$ mice were on a DKD-resistant mixed C57BL/6J background, unilateral nephrectomy was performed 1 week before diabetes induction with STZ, and only male mice were used, because they are more susceptible to DKD than are female mice. Unilateral nephrectomy was performed on anesthetized mice when they were 7 weeks old (Gpr56$^{+/+}$ and Gpr56$^{-/-}$ mice), as previously described (24). One week after surgery, mice were randomly divided into two groups for injection of low-dose STZ (50 mg/kg) or citrate buffer for five consecutive days (n = 12 mice/group). Blood glucose levels were measured 48 h after the injection and monitored biweekly thereafter, using the Accu-Chek Aviva glucometer (Roche Diabetes Care, Indianapolis, IN) from tail-vein blood samples. Only the animals with blood glucose concentrations >16.7 mmol/L were considered diabetic. All mice were sacrificed at 20 weeks after STZ injection. From each group of 12 mice, the kidneys of six mice were collected and used for histologic analysis, and kidneys from the remaining six mice were used for glomerular isolation. All mouse procedures were performed according to the protocol approved by the Institutional Animal Care and Use Committee of the Icahn School of Medicine at Mount Sinai (IACUC-2018-0033).

Urine Albumin Measurements

For the determination of urinary albumin excretion, 24-h urine collections from animals in the metabolic cages were analyzed for total albumin content using a commercial ELISA kit (Bethyl Laboratory Inc., Houston, TX) according to the manufacturer's instructions.

Measurement of Blood Pressure

Blood pressure was measured using the noninvasive tail-cuff blood pressure system (Kent Scientific, Torrington,

CT). Mice were first acclimated to the tail-cuff manometer and restraining device for 10–20 min/day for at least 3 days before actual data acquisition.

Kidney Histology

Kidney samples were fixed in 10% formalin, embedded in paraffin, and sectioned to 5-μm thickness. Sections were stained with periodic acid Schiff for analysis of glomerular area and mesangial matrix expansion. Images were taken at ×100 to ×400 magnification using a Zeiss AX10 microscope (Carl Zeiss Jena, Toronto, Canada). The relative mesangial area was expressed as a percentage of mesangial-to-glomerular surface area. Assessment of the mesangial and glomerular cross-sectional areas was performed in a blinded fashion by pixel counts on a minimum of 30 glomeruli per section under ×200 magnification (Zeiss AX10 microscope). For transmission electron microscopy, kidney cortex samples fixed in 2.5% glutaraldehyde were divided into sections and mounted on a copper grid; images were acquired using a Hitachi H7650 microscope (Hitachi, Tokyo, Japan).

Immunofluorescence and Immunohistochemical Staining

Immunofluorescence staining was conducted on frozen or paraffin kidney sections using standard procedures. Primary antibodies used were anti-GPR56 (MABN310; Sigma), anti-CD31 (550274; BD Bioscience), anti-nephrin (NBP1-30130; Novus Biologicals), anti–8-oxo-dG (ab48508; Abcam), anti–eNOS (612392; BD Biosciences), and anti-WT1 (sc-7385M; Santa Cruz). Slides were counterstained with 6-diamidino-2-phenylindole, and mounted with Aqua PolyMount (Polysciences Inc., Warrington, PA). Images were acquired using an AxioVision II microscope with a digital camera (Carl Zeiss). For immunohistochemical staining of GPR56, deparaffinized kidney sections were incubated with anti-GPR56 antibody (720373; Fisher Scientific). After washing, sections were incubated with an anti-rabbit biotinylated secondary antibody at room temperature and then with the avidin-biotin-peroxidase complex (Vectastain Elite ABC Kit; Vector Laboratories, Burlingame, CA). The reaction products were developed using the 3,3′-diaminobenzidine substrate and mounted.

Statistical Analysis

Data are expressed as mean ± SD. For comparisons of means between the two groups, a two-tailed Welch *t* test was performed. For comparison of means among 3 or more groups, ANOVA with Bonferroni modification was applied. Prism software (version 9; GraphPad, La Jolla, CA) was used for statistical analyses.

Data and Resource Availability

The data sets generated during and/or analyzed during this study are available from the corresponding authors upon reasonable request.

RESULTS

GPR56 Is Increased in GECs in Mouse and Human Diabetic Kidneys

Using an unbiased transcriptomic analysis of GECs derived from control and eNOS-deficient diabetic mice, we previously identified *Gpr56* as one of the highly upregulated genes in GECs in the early DKD (12), as shown in Fig. 1*A*. In addition, querying of independent mouse glomerular small conditional RNA-sequencing data sets confirmed the predominant expression of *Gpr56* in GECs among all glomerular cells (25,26) (Fig. 1*B* and *C* and Supplementary Fig. 1*A*) and its increase in the diabetic mice (Fig. 1*B* and *C*). Outside the glomerular compartment, *Gpr56* expression was found also in the distal tubules (27) (Supplementary Fig. 1*B*). Immunostaining of GPR56 protein with an endothelial marker (CD31) of eNOS-deficient diabetic mice showed colocalization of GPR56 with CD31 (Fig. 1*D*), confirming the predominant increase of GPR56 in GECs among the glomerular cells in the diabetic kidneys. Interestingly, increased glomerular *GPR56* expression in human diabetic kidneys was negatively correlated with the estimated glomerular filtration rate in DKD (Fig. 1*E–G*, obtained from nephroseq.org). Increased glomerular expression of GPR56 protein was also observed in human DKD biopsy samples in comparison with normal controls (i.e., normal areas of nephrectomy samples) (Fig. 1*H* and *I*), consistent with the above findings.

We previously demonstrated that the *Gpr56* expression is induced in cultured mouse GECs under high-glucose conditions (12), suggesting that hyperglycemia may contribute to its increased expression in diabetes. Because the accumulation of advanced glycation end products (AGEs) is another common feature in diabetes, we examined whether AGEs may affect GPR56 expression in cultured GECs. Incubation of increasing concentrations of AGE-modified BSA (AGE-BSA) with GECs in culture for 24 h significantly enhanced the expression of GPR56 mRNA and protein in comparison with incubation with control BSA (Fig. 2*A–C*). These data suggest that hyperglycemic conditions and accumulated AGEs contribute to the enhanced GPR56 expression in GECs in diabetic kidneys.

GPR56 Suppresses eNOS Phosphorylation and Expression in GECs Through the Coupling of $G\alpha_{12/13}$ and $G\alpha i$ Pathways

We next examined the effects of change in GPR56 expression and activation in cultured mGECs. Stable GPR56 knockdown in mGECs was achieved by lentiviral transduction of vector expressing shRNA sequences against *Gpr56* (short hairpin Gpr56 [shGpr56]) (12), which resulted in an approximately 60% reduction in *Gpr56* mRNA in comparison with controls cells expressing shScr sequences (Fig. 3*A*). Because ligand activation of GPR56 by ECM molecules, such as collagen III, results in $G\alpha_{12/13}$-mediated RhoA activation (20), and RhoA and Rho kinase (ROCK) activation is associated with decreased eNOS phosphorylation to affect endothelial homeostasis (28), we next examined whether GPR56-mediated $G\alpha_{12/13}$/RhoA activation would change eNOS phosphorylation

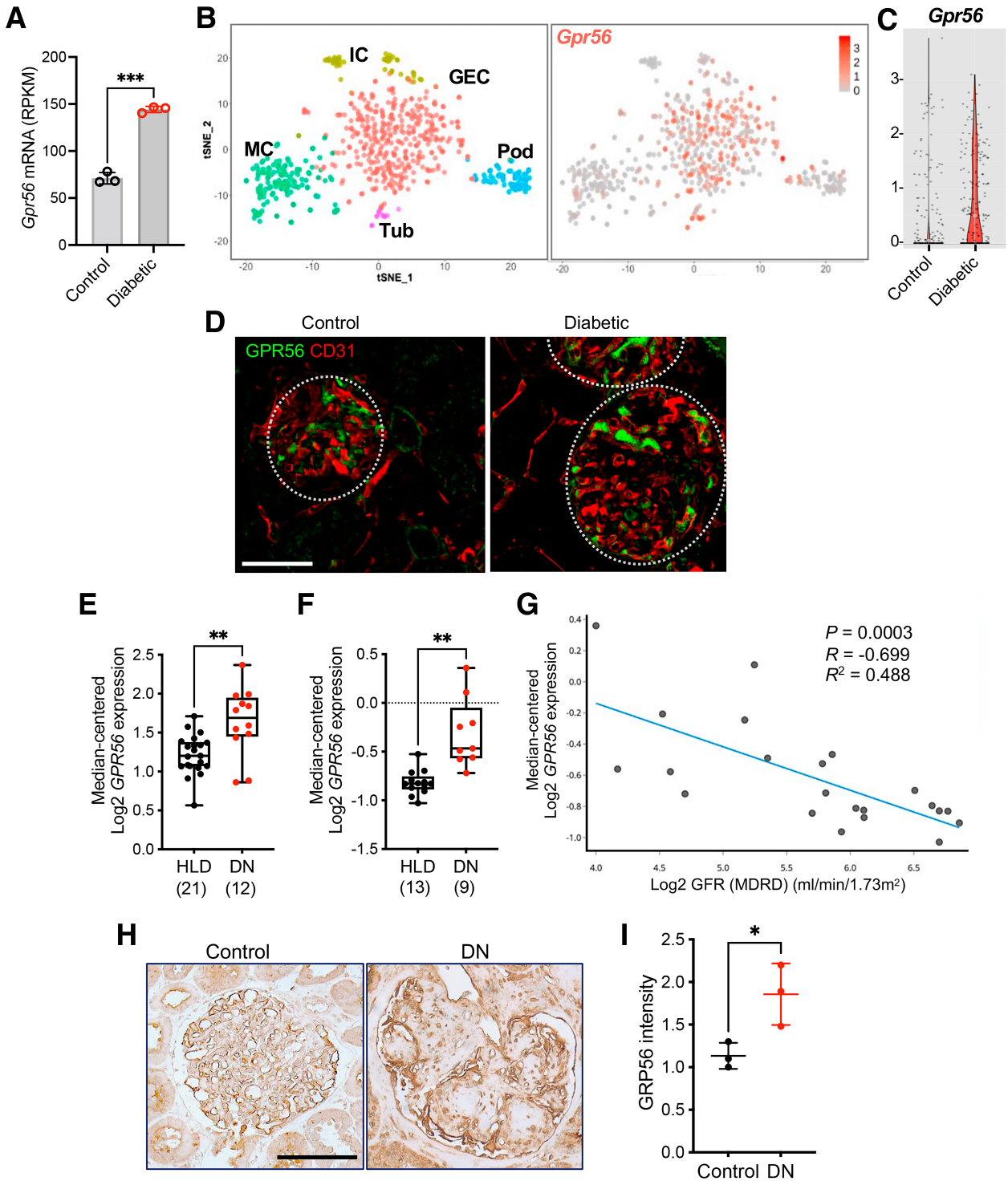

Figure 1—Glomerular GPR56 expression is increased in DKD. *A*: *Gpr56* expression from bulk RNA-sequencing data of isolated GECs (12) show elevated *Gpr56* mRNA expression in diabetic mice. Each sample represents isolated GECs pooled from three or four mice. RPKM, reads per kilobase per million. ***$P < 0.001$ when compared between two groups by two-tailed Welch's *t* test. *B* and *C*: Small conditional RNA-sequencing analysis of glomerular cells (25) shows an enriched expression of *Gpr56* in GECs (*B*) and enhanced expression in diabetic mouse GECs (*C*). Gene expression is shown on a log scale, and each dot represents a single GEC. *D*: Representative images of GPR56 (green) costained with CD31 (red) of control and diabetic eNOS-null mouse kidneys. Scale bar: 50 μm. *E* and *F*: *GPR56* mRNA expression in microdissected glomeruli samples from diabetic nephropathy (DN) and healthy living donors (HLD) in the Ju chronic kidney disease (CKD) glom data set (GSE47185, *E*) and Woroniecka diabetes glom data set (GSE30122, *F*) from the Nephroseq database (nephroseq.org). The sample size of each group is shown in parentheses. **$P < 0.01$ between two groups by Welch's *t* test. *G*: Pearson correlation analysis between *GPR56* mRNA expression and estimated glomerular filtration rate in DN (nephroseq.org; data set GSE30122). *H*: Representative images of GPR56 immunostaining in glomeruli of control nephrectomy specimen (control) and DN biopsy samples. Scale bar: 100 μm. *I*: Quantification of optical density of GPR56 immunostaining ($n = 3$ patient samples/group) in arbitrary units. *$P < 0.05$ between two groups by unpaired *t* test.

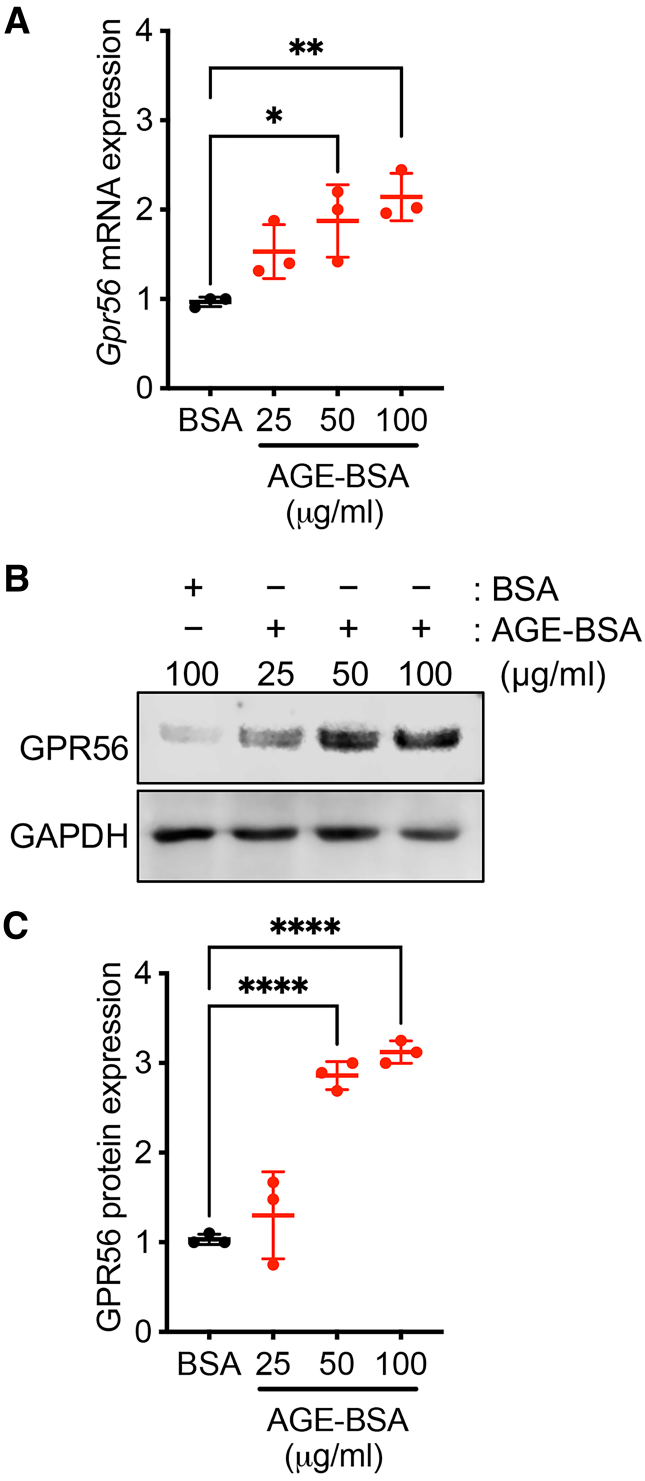

Figure 2—GPR56 expression is increased in cultured mGECs by exposure to AGE products. mGECs were treated with normal BSA or glycated BSA (AGE-BSA) for 24 h. *A*: Real-time PCR analysis shows the change in *Gpr56* mRNA expression with AGE-BSA treatment (25, 50, or 100 μg/mL) compared with control BSA treatment (100 μg/mL). *B*: Western blot analysis of GECs with BSA or AGE-BSA treatment. A representative image is shown of three experiments. *C*: Densitometric analysis of GPR56 protein expression in (*B*), shown as fold change to control BSA. *$P < 0.05$, **$P < 0.01$, ****$P < 0.0001$ between indicated groups by one-way ANOVA with Bonferroni correction.

in mGECs. Upon brief stimulation with recombinant collagen III, shScr GECs showed a marked reduction in eNOS phosphorylation (Ser-1177), but this effect was abrogated in shGpr56 GECs (Fig. 3*B*). We also tested the effects of stable overexpression of Gpr56 (Gpr56^{ov}) in mGECs by lentiviral transduction, which led to approximately a fivefold increase in *Gpr56* transcript in comparison with control vector–transduced cells (Fig. 3*C*). Upon stimulation with collagen III, a substantial reduction in eNOS phosphorylation was observed in Gpr56^{ov} mGECs in comparison with control cells, and this effect was abolished in the presence of the ROCK inhibitor HA-1077 (Fasudil) (Fig. 3*D*). These effects of GPR56 knockdown and overexpression in mGECs are consistent with the coupling of $G\alpha_{12/13}$/RhoA by GPR56 to suppress eNOS phosphorylation and activity.

In addition to $G\alpha_{12/13}$-mediated RhoA activation, GPR56 has been shown to activate $G\alpha_i$ signaling (22). Therefore, we also tested whether GPR56 expression would influence the cAMP levels in mGECs. The control, Gpr56^{ov}, and shGpr56 mGECs were stimulated with a β-adrenergic agonist, fenoterol, which led to a robust cAMP accumulation in all cell types (Fig. 3*E*); however, the cAMP accumulation was sustained in Gpr56^{ov} cells and, conversely, it was significantly reduced in shGpr56 knockdown cells (Fig. 3*E*), indicating that GPR56 negatively regulates cAMP/PKA signaling in mGECs. cAMP/PKA signaling is implicated in the regulation of transcription factor KLF4 expression in various cell types (29–31), and KLF4 is one of the key transcription factors for endothelial homeostasis and a potent inducer of eNOS expression (32,33). Therefore, we next examined whether GPR56 would negatively influence KLF4 expression via $G\alpha_i$-mediated inhibition of cAMP/PKA signaling in mGECs. As shown in Fig. 3*F*, the stable overexpression of KLF4, indeed, resulted in enhanced eNOS expression in mGECs, and KLF4 and eNOS expression were both upregulated in shGpr56 mGECs in comparison with control shScr (Fig. 3*G*; −H89), but this effect was markedly diminished in the presence of PKA antagonist, H89 (Fig. 3*G*; +H89). Together, these results suggest that the acute stimulation of GPR56 through collagen III leads to phosphorylation of eNOS via $G\alpha_{12/13}$-mediated RhoA activation, and GPR56 further controls the total expression of eNOS over time via $G\alpha_i$ coupling and inhibition of cAMP/PKA pathway, resulting in reduced transcription of KLF4.

Loss of GPR56 Attenuates Albuminuria and Glomerulopathy in Diabetic Mice

Given these salient roles of GPR56 in eNOS regulation in GECs, we next explored the effects of GPR56 loss in DKD progression in vivo. *Gpr56*-null (*Gpr56*$^{-/-}$) mice on the mixed C57BL/6J background were viable and without gross defects. Western blot analysis confirmed the loss of GPR56 in the kidneys of *Gpr56*$^{-/-}$ mice (Supplementary Fig. 2*A*); no defects in renal function (data not shown) or overall kidney histology were observed up to 8 months of age (Supplementary Fig. 2*B*). Because *Gpr56*$^{-/-}$ mice were on a

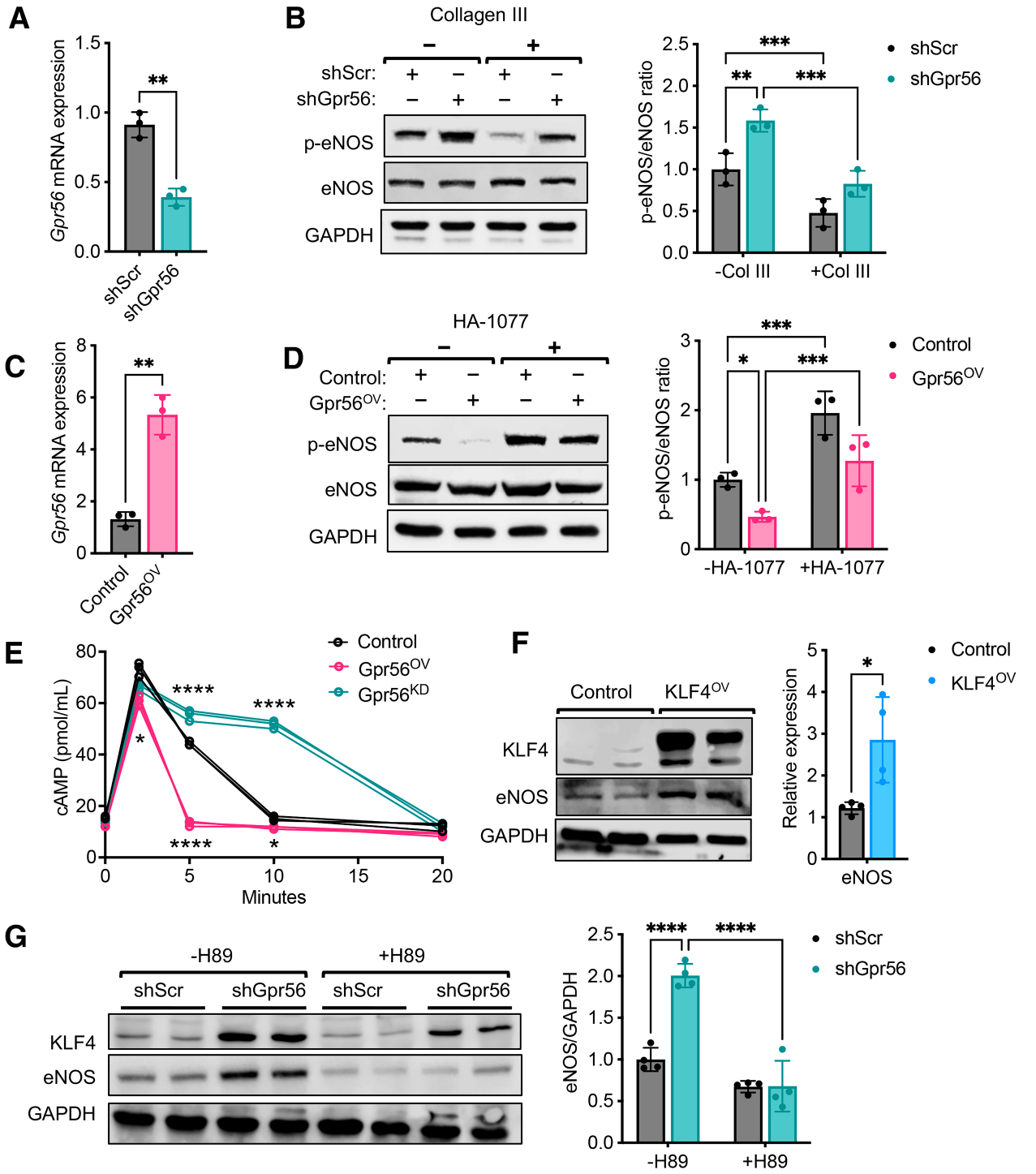

Figure 3—GPR56 suppresses eNOS phosphorylation and expression via the PKA/KLF4 pathway. *A*: *Gpr56* expression was assessed by real-time PCR in mGECs stably transduced with lentivirus expressing shScr or ShGpr56. $^{**}P < 0.01$ between two groups by unpaired *t* test. *B*: mGECs were stimulated with collagen III for 10 min, and lysates were probed for phosphorylated and total eNOS (p-eNOS and eNOS). Densitometric analysis is shown on the right. $^{**}P < 0.01$ and $^{***}P < 0.001$ between indicated groups by two-way ANOVA with Bonferroni correction. *C*: *Gpr56* expression was assessed by real-time PCR in mGECs stably transduced with control or GPR56^{OV} lentiviral vectors. *D*: mGECs were preincubated with or without selective ROCK inhibitor (HA-1077; 50 μmol/L) for 24 h before collagen stimulation, and lysates were probed for eNOS (p-eNOS and eNOS). Densitometric analysis is shown on the right. $^{*}P < 0.01$ and $^{***}P < 0.001$ between indicated groups by two-way ANOVA with Bonferroni correction. *E*: mGECs were treated with fenoterol (1 μmol/L) and cAMP production was measured by ELISA ($n = 3$/group). $^{*}P < 0.05$ and $^{****}P < 0.0001$ vs. control by two-way ANOVA with Bonferroni correction. *F*: mGECs were stably transduced with control or KLF4 overexpression (KLF4^{OV}) lentiviral vectors, and lysates were probed for KLF4 and eNOS expression. Densitometric analysis is shown on the right for relative eNOS expression normalized to GAPDH. $^{*}P < 0.05$ between two groups by unpaired *t* test. *G*: mGECs were incubated with PKA inhibitor (H89; 10 μmol/L) for 24 h, and lysates were probed for KLF4 and eNOS expression. Densitometric analysis is shown on the right for relative eNOS expression normalized to GAPDH. $^{****}P < 0.0001$ between indicated groups by two-way ANOVA with Bonferroni correction.

relatively DKD-resistant mixed background, we first performed a unilateral nephrectomy in *Gpr56*$^{+/+}$ and *Gpr56*$^{-/-}$ mice 1 week before diabetes induction by STZ to aggravate the ensuing diabetic kidney injury (34) (Supplementary Fig. 3*A*). Uninephrectomized *Gpr56*$^{+/+}$ and *Gpr56*$^{-/-}$ mice with vehicle injection (−STZ) were used as nondiabetic controls, and all mice were euthanized after 20 weeks after diabetes induction. The resulting hyperglycemia, weight loss, and elevation in blood pressure were similar between diabetic *Gpr56*$^{+/+}$ and *Gpr56*$^{-/-}$ mice (Supplementary Fig. 3*B–D*). However, diabetes-induced kidney hypertrophy and albuminuria were significantly reduced in the *Gpr56*$^{-/-}$ mice in comparison with *Gpr56*$^{+/+}$ mice (Fig. 4*A* and *B*). Histological analysis also showed significant attenuation in the mesangial matrix accumulation and glomerular hypertrophy in the diabetic *Gpr56*$^{-/-}$ mice in comparison with the diabetic *Gpr56*$^{+/+}$ mice (Fig. 4*C* and *D*). The ultrastructural analyses by transmission electron microscopy

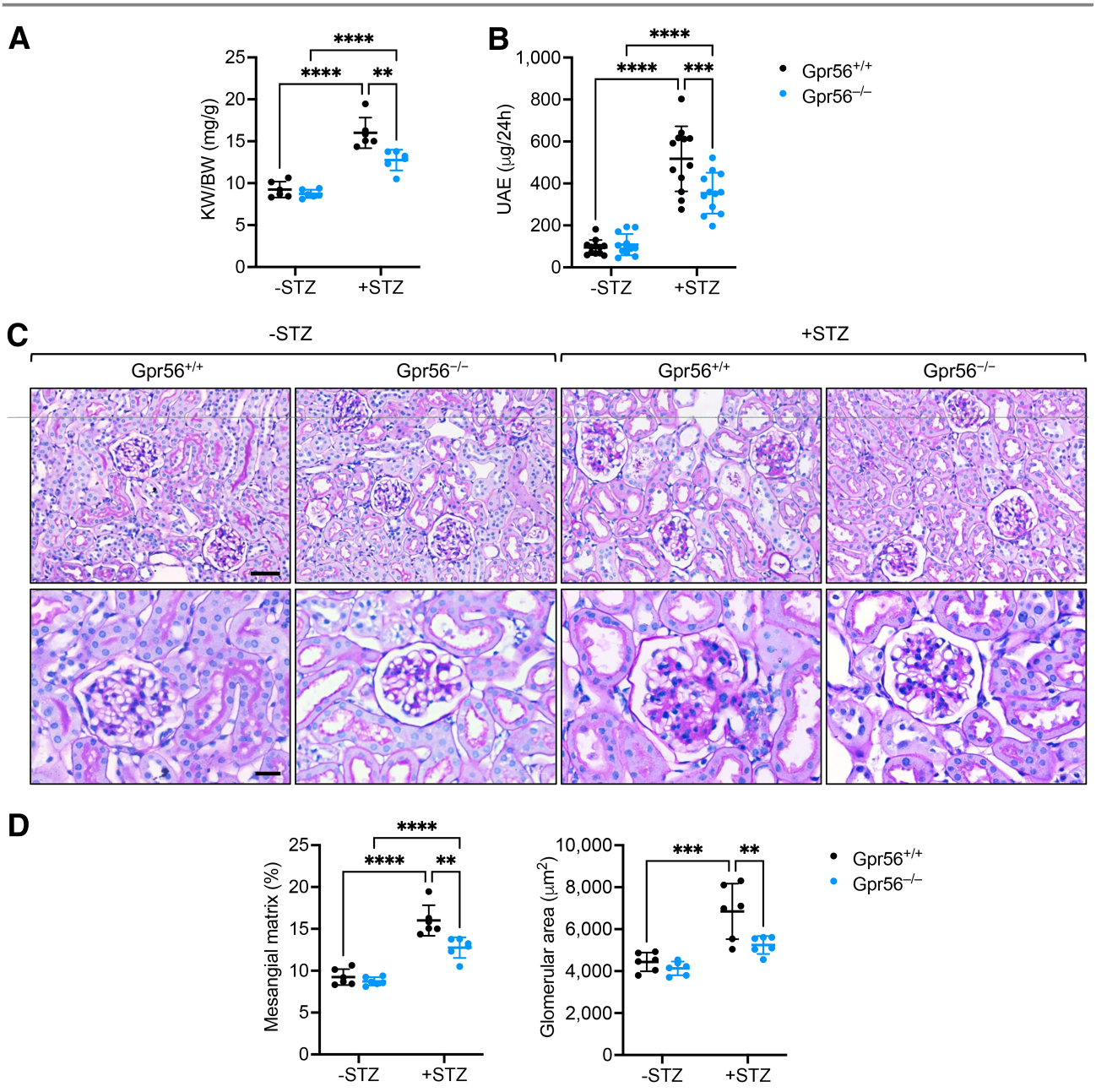

Figure 4—GPR56 loss attenuates STZ-induced DKD in mice. *A*: The kidney weight to body weight (KW/BW) ratio was determined at 20 weeks after STZ induction (n = 6 mice/group). *B*: The 24-h total urinary albumin excretion of control and diabetic mice (n = 12). *C*: Representative images of periodic acid Schiff–stained kidney sections of control and diabetic mice at ×200 and ×400 magnifications (scale bars: 50 μm, upper panels; 20 μm, lower panels). *D*: Quantification of glomerular area and mesangial matrix area is shown (n = 6 mice/group). $^{**}P < 0.01$, $^{***}P < 0.001$, and $^{****}P < 0.0001$ when compared between indicated groups by two-way ANOVA with Bonferroni correction.

also showed a greater extent of podocyte foot process effacement in the diabetic *Gpr56*$^{+/+}$ mice than in the diabetic *Gpr56*$^{-/-}$ mice (Fig. 5*A*). In line with these findings, the diabetes-induced reduction of podocytes, as ascertained by the number of WT1^{+} cells per glomerular cross-section, was much more pronounced in *Gpr56*$^{+/+}$ mice than in *Gpr56*$^{-/-}$ mice (Fig. 5*B* and *C*). Together, these results demonstrated the attenuation of diabetic glomerulopathy by GPR56 loss in vivo.

Loss of GPR56 Restores KLF4 and eNOS Expression in GECs of Diabetic Mice

Given the marked protection against DKD by GPR56 loss, we assessed the expression levels of KLF4 and eNOS in GECs of diabetic mice. Quantitative PCR analysis of *Klf4* and *Nos3* mRNA in isolated glomeruli of control and diabetic mice indeed showed that loss of GPR56 elevated the expression of both genes in control and diabetic mice (Fig. 6*A*). Although diabetes reduced their expression,

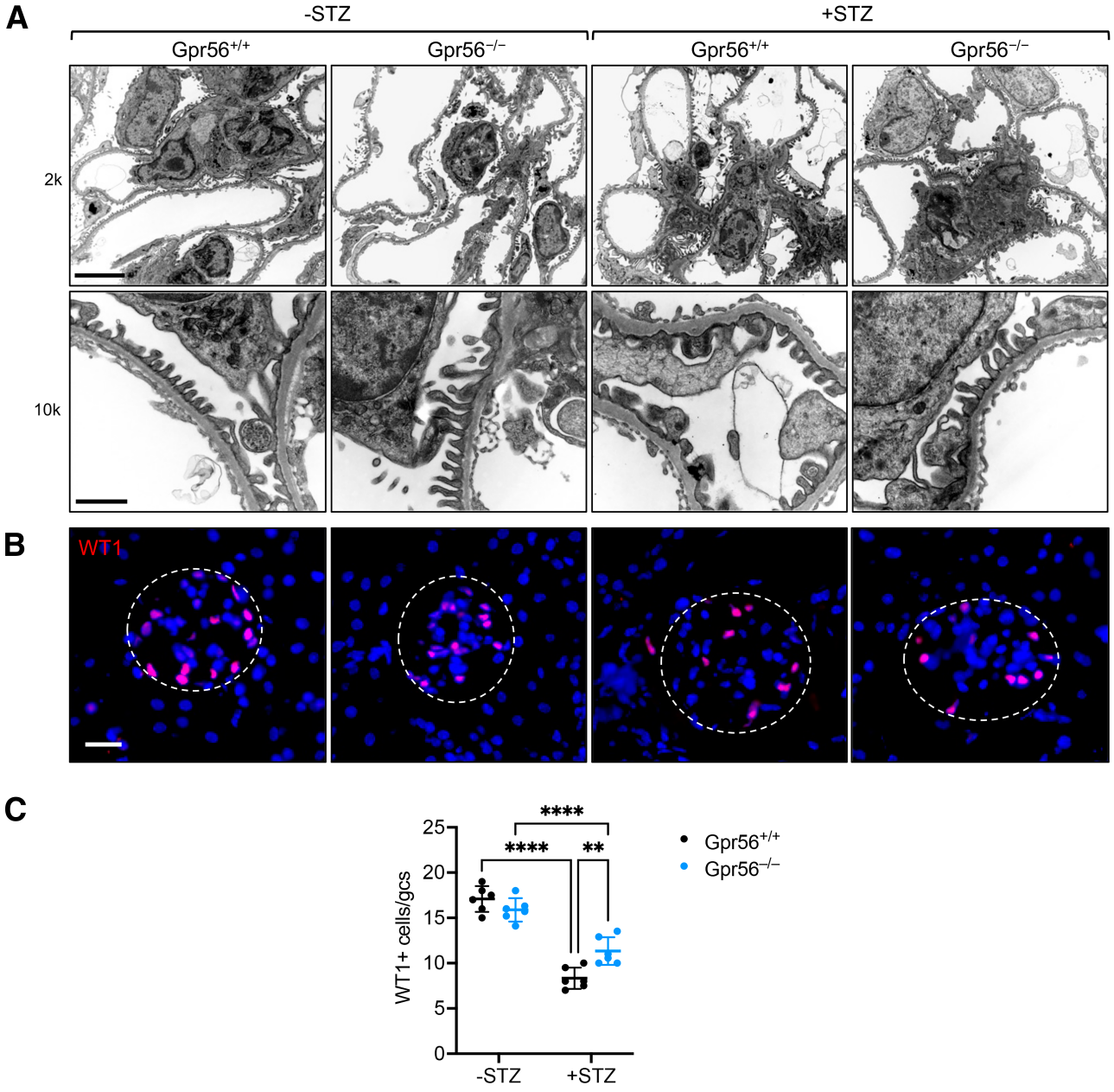

Figure 5—GPR56 loss attenuates podocyte injury in diabetic mice. *A*: Representative transmission electron microscopy images of control and diabetic mice at ×2,000 and ×10,000 magnifications. Scale bars: 5 μm, upper panel; 1 μm, lower panel. *B*: Representative images of WT1^{+} cells in glomeruli of control and diabetic mice. Scale bar: 20 μm. *C*: Quantification of WT1^{+} cells per glomerular cross-section (gcs; n = 6 mice/group; n = 20–30 glomeruli evaluated per mouse). $^{**}P < 0.01$ and $^{****}P < 0.0001$ when compared between indicated groups by two-way ANOVA with Bonferroni correction.

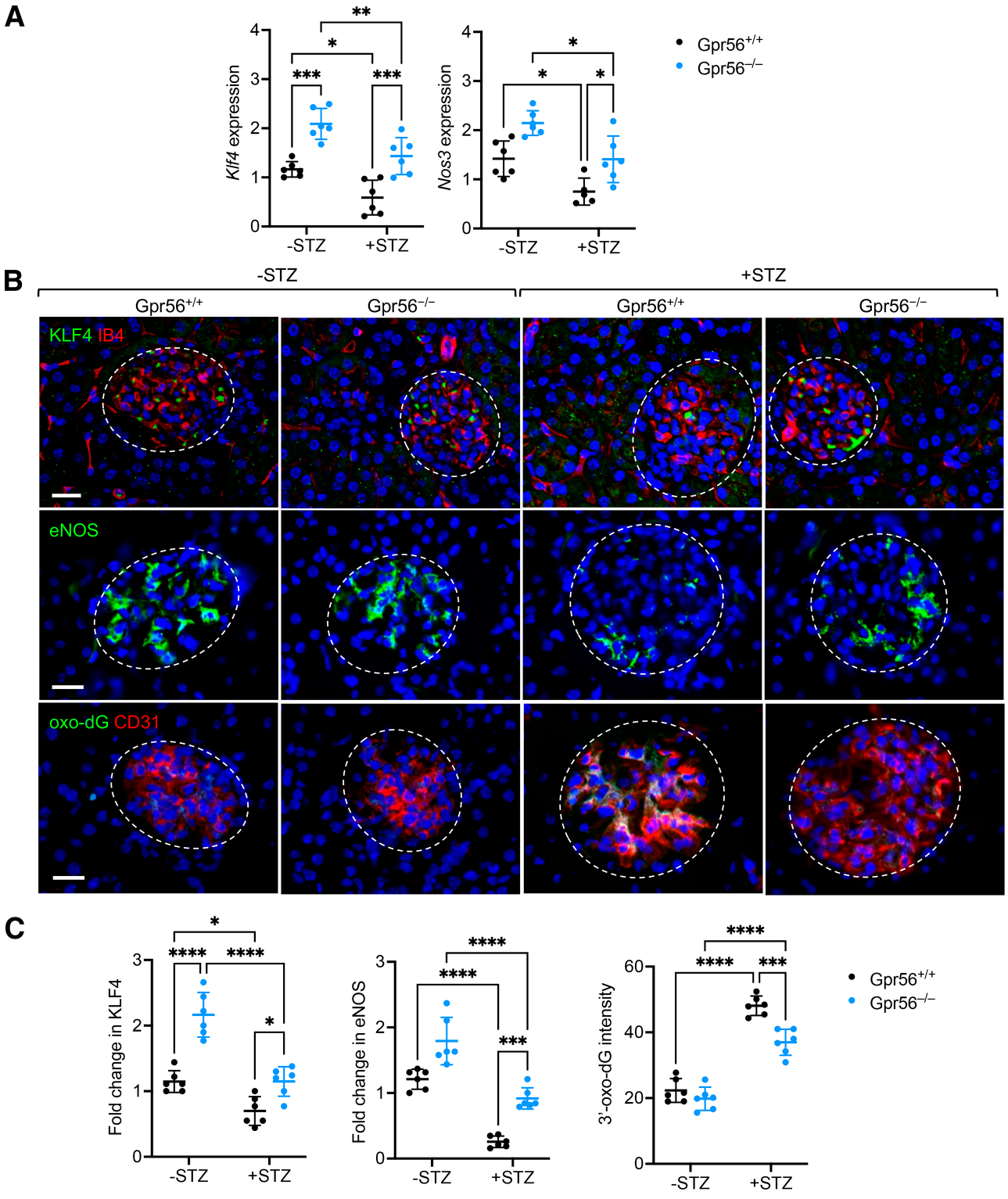

Figure 6—GPR56 loss increases glomerular endothelial expression of eNOS and KLF4 in diabetic mice. *A*: *Nos3* and *Klf4* mRNA in isolated glomeruli of control and diabetic mice. *B*: Representative images of KLF4, eNOS, and 8-oxo-dG immunostaining in the glomeruli of control and diabetic mice. Endothelial cells are costained with IB4 or CD31, and DNA is counterstained with DAPI. Scale bar: 20 μm. *C*: Quantification of Klf4, eNOS, and 8-oxo-dG intensity (in arbitrary units) in glomeruli of control and diabetic mice (n = 6 mice/group; n = >30 glomeruli evaluated per mouse). *$P < 0.05$, ***$P < 0.001$, and ****$P < 0.0001$ when compared between indicated groups by two-way ANOVA with Bonferroni correction.

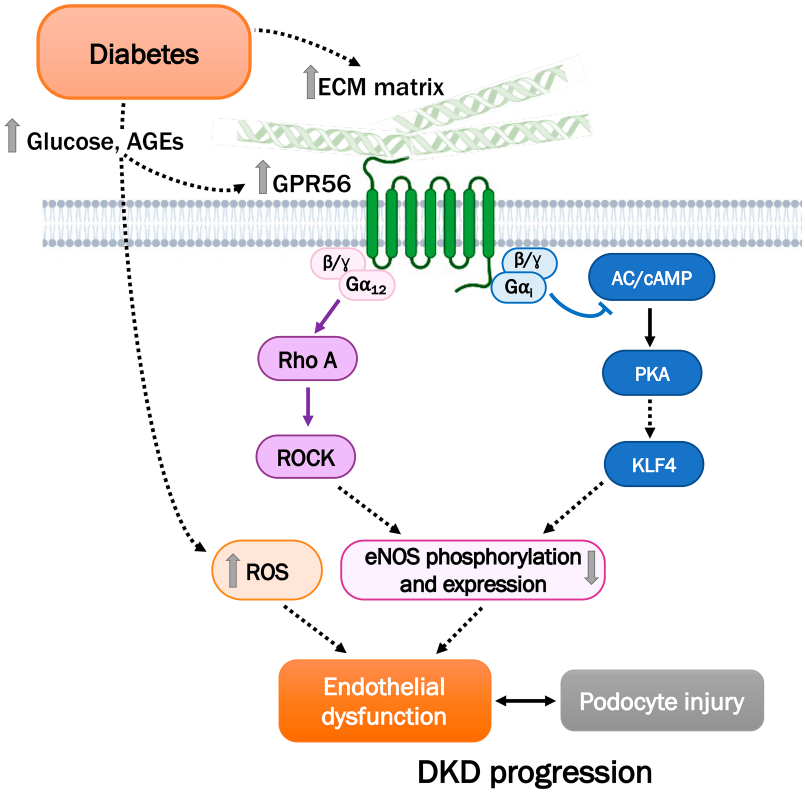

Figure 7—Schematic of GPR56-mediated GEC dysfunction in DKD. High glucose levels and increased AGE products contribute to the enhanced levels of GPR56 and reactive oxygen species (ROS). GPR56 elicits $G\alpha_{12/13}$-mediated RhoA activation and Gαi-mediated inhibition of the cAMP/PKA pathway in GECs to result in eNOS dysregulation. AC, adenylyl cyclase.

these gene levels in diabetic *Gpr56*$^{-/-}$ mice were comparable to those observed in control *Gpr56*$^{+/+}$ mice (Fig. 6*A*). We further confirmed these findings by immunofluorescence (Fig. 6*B* and *C*), which showed that loss of GPR56 restored the expression of KLF4 and eNOS in diabetic mice. Moreover, because the accumulation of reactive oxygen species in kidney cells, particularly in GECs, plays a key role in DKD pathogenesis (35–37), we examined the extent of oxidative stress in the GECs of diabetic mice. Using the detection of 8-oxo-2′-deoxyguanosine (8-oxo-dG) as a surrogate marker of oxidative stress and endothelial marker CD31, we observed that although diabetes markedly increased the level of oxidative stress in GECs of both *Gpr56*$^{+/+}$ and *Gpr56*$^{-/-}$ mice, it was significantly mitigated in the diabetic *Gpr56*$^{-/-}$ mice (Fig. 6*B* and *C*). Therefore, taken together, these results indicate that the loss of GPR56 attenuates diabetic glomerulopathy and that this is due, in part, the attenuation of diabetes-induced GEC dysfunction by restoring KLF4 and eNOS expression in vivo.

DISCUSSION

Although glomerular endothelial dysfunction is well established as playing a key role in early DKD pathogenesis, because of the heterogeneity of kidney endothelial cells, the full mechanistic insight in molecular and cellular pathways affected by diabetes specifically in GECs is not entirely understood. Our recent transcriptomic analysis of isolated GECs from control and diabetic mice offers in-depth gene expression analysis occurring specifically in GECs (12) that can be used in a complementary manner with single-cell transcriptomic analysis of kidney cells from diabetic mice (13). GPR56 was one of the highly expressed genes in GECs of diabetic mice, but it did not have an established role in kidney disease settings. Our previous and current results indicate that GPR56 expression is induced in diabetic conditions (i.e., by high glucose levels and AGE products) and that its expression is increased in GECs in mouse and human diabetic kidneys. As an adhesion GPCR, GPR56 can be activated in response to the laminar shear stress (22). Thus, it is plausible that in addition to enhanced expression, its activity is further increased in GECs that are exposed to increased shear stress in the setting of glomerular hyperfiltration (38), as well as accumulation of its ECM ligands in DKD.

As an adhesion GPCR, GPR56 elicits $G\alpha_{12/13}$-mediated RhoA activation (20). The RhoA/ROCK pathway is a critical regulator of endothelial cell function, such as eNOS activity, vascular permeability, and angiogenesis (28), and because eNOS deficiency promotes DKD progression (39), in this study we explored the potential role of GPR56 on eNOS regulation in GECs in DKD. The results from our study demonstrate that GPR56-mediated RhoA/ROCK activation leads to decreased eNOS phosphorylation and expression in GECs (Fig. 7). Moreover, because another purported function of

GPR56 is Gαi-mediated inhibition of cAMP/PKA pathway (21), we examined whether activation of GPR56 resulted in cAMP accumulation in GECs. We now provide evidence that GPR56 couples to Gαi, resulting in reduced cAMP/PKA signal transduction, thereby decreasing KLF4 and eNOS expression in GECs. In addition to the regulation of eNOS expression, KLF4 is shown to confer anti-inflammatory effects in endothelial cells (32). Because GPR56 loss results in enhanced KLF4 expression and reduced oxidative stress in GECs of diabetic kidneys, it is likely that these effects contribute to the overall reduction of endothelial inflammation and dysfunction to attenuate DKD in vivo.

Nevertheless, because GPR56 expression is not limited to GECs, and global *Gpr56*-null mice were used for the study, the significant attenuation in DKD phenotype in the diabetic $Gpr56^{-/-}$ mice is unlikely to be solely due to its role in GECs. However, given that GPR56 expression is largely restricted to GECs in the glomeruli, and its loss resulted in enhanced eNOS expression with diminution of oxidative stress in GECs of diabetic mice, these demonstrate a key role of GPR56 in GECs to promote DKD. The loss of GPR56 not only attenuated GEC injury but also resulted in reduced podocyte damage, albuminuria, and overall diabetic glomerulopathy, underscoring the important glomerular cell cross-talk in DKD progression. Because Gpr56-null mice were without any gross defects, pharmacological inhibition of GPR56 may be a viable therapeutic approach against DKD.

In summary, our study demonstrates a salient role of GPR56 in GEC dysfunction in DKD progression and suggests that targeting of GPR56 may impede the progression of DKD.

Funding. J.F. is supported by the National Institutes of Health (NIH) National Institute of Diabetes and Digestive and Kidney Diseases (NIDDK) grant K01DK125614-01A1; J.C.H. is supported by NIH NIDDK grants R01DK109683, R01DK122980, R01DK129467, and P01DK56492, and VA Merit Award I01BX000345; K.L. is supported by NIH NIDDK grants R01DK117913-01, R01DK129467, and R01DK133912.

Duality of Interest. No potential conflicts of interest relevant to this article were reported.

Author Contributions. Z.W., J.C.H., K.L., and J.F. conceived and designed the experiments; J.W., M.C., X.W., B.L., and J.F. performed the experiments and the data analysis; and Z.W., Q.L., J.C.H., K.L., and J.F. drafted and revised the manuscript. J.C.H. and K.L. are the guarantors of this work and, as such, had full access to all the data in the study and take responsibility for the integrity of the data and the accuracy of the data analysis.

References

1. Osterby R, Nyberg G. New vessel formation in the renal corpuscles in advanced diabetic glomerulopathy. J Diabet Complications 1987;1:122–127
2. Nyengaard JR, Rasch R. The impact of experimental diabetes mellitus in rats on glomerular capillary number and sizes. Diabetologia 1993;36:189–194
3. Guo M, Ricardo SD, Deane JA, Shi M, Cullen-McEwen L, Bertram JF. A stereological study of the renal glomerular vasculature in the db/db mouse model of diabetic nephropathy. J Anat 2005;207:813–821
4. Karalliedde J, Gnudi L. Endothelial factors and diabetic nephropathy. Diabetes Care 2011;34(Suppl. 2):S291–S296
5. Yuen DA, Stead BE, Zhang Y, et al. eNOS deficiency predisposes podocytes to injury in diabetes. J Am Soc Nephrol 2012;23:1810–1823
6. Zhao HJ, Wang S, Cheng H, et al. Endothelial nitric oxide synthase deficiency produces accelerated nephropathy in diabetic mice. J Am Soc Nephrol 2006;17:2664–2669
7. Nakagawa T, Sato W, Glushakova O, et al. Diabetic endothelial nitric oxide synthase knockout mice develop advanced diabetic nephropathy. J Am Soc Nephrol 2007;18:539–550
8. Satchell SC, Tooke JE. What is the mechanism of microalbuminuria in diabetes: a role for the glomerular endothelium? Diabetologia 2008;51:714–725
9. Haraldsson B, Nyström J. The glomerular endothelium: new insights on function and structure. Curr Opin Nephrol Hypertens 2012;21:258–263
10. Stehouwer CD, Fischer HR, van Kuijk AW, Polak BC, Donker AJ. Endothelial dysfunction precedes development of microalbuminuria in IDDM. Diabetes 1995;44:561–564
11. Weil EJ, Lemley KV, Mason CC, et al. Podocyte detachment and reduced glomerular capillary endothelial fenestration promote kidney disease in type 2 diabetic nephropathy. Kidney Int 2012;82:1010–1017
12. Fu J, Wei C, Zhang W, et al. Gene expression profiles of glomerular endothelial cells support their role in the glomerulopathy of diabetic mice. Kidney Int 2018;94:326–345
13. Fu J, Wang X, Sun Z, et al. The single-cell landscape of kidney cells from mice with early diabetic kidney disease. Kidney Int 2022;102:1291–1304
14. Hong Q, Zhang L, Fu J, et al. LRG1 promotes diabetic kidney disease progression by enhancing TGF-β-induced angiogenesis. J Am Soc Nephrol 2019;30:546–562
15. Ganesh RA, Venkataraman K, Sirdeshmukh R. GPR56: an adhesion GPCR involved in brain development, neurological disorders and cancer. Brain Res 2020;1747:147055
16. Singh AK, Lin HH. The role of GPR56/ADGRG1 in health and disease. Biomed J 2021;44:534–547
17. Xu L. GPR56 interacts with extracellular matrix and regulates cancer progression. Adv Exp Med Biol 2010;706:98–108
18. Luo R, Jeong SJ, Yang A, et al. Mechanism for adhesion G protein-coupled receptor GPR56-mediated RhoA activation induced by collagen III stimulation. PLoS One 2014;9:e100043
19. Luo R, Jeong SJ, Jin Z, Strokes N, Li S, Piao X. G protein-coupled receptor 56 and collagen III, a receptor-ligand pair, regulates cortical development and lamination. Proc Natl Acad Sci USA 2011;108:12925–12930
20. Iguchi T, Sakata K, Yoshizaki K, Tago K, Mizuno N, Itoh H. Orphan G protein-coupled receptor GPR56 regulates neural progenitor cell migration via a G alpha 12/13 and Rho pathway. J Biol Chem 2008;283:14469–14478
21. Stoveken HM, Hajduczok AG, Xu L, Tall GG. Adhesion G protein-coupled receptors are activated by exposure of a cryptic tethered agonist. Proc Natl Acad Sci USA 2015;112:6194–6199
22. Yeung J, Adili R, Stringham EN, et al. GPR56/ADGRG1 is a platelet collagen-responsive GPCR and hemostatic sensor of shear force. Proc Natl Acad Sci USA 2020;117:28275–28286
23. Yang L, Chen G, Mohanty S, et al. GPR56 regulates VEGF production and angiogenesis during melanoma progression. Cancer Res 2011;71:5558–5568
24. Zhong F, Mallipattu SK, Estrada C, et al. Reduced Krüppel-like factor 2 aggravates glomerular endothelial cell injury and kidney disease in mice with unilateral nephrectomy. Am J Pathol 2016;186:2021–2031
25. Fu J, Akat KM, Sun Z, et al. Single-cell RNA profiling of glomerular cells shows dynamic changes in experimental diabetic kidney disease. J Am Soc Nephrol 2019;30:533–545
26. Karaiskos N, Rahmatollahi M, Boltengagen A, et al. A single-cell transcriptome atlas of the mouse glomerulus. J Am Soc Nephrol 2018;29:2060–2068
27. Wu H, Kirita Y, Donnelly EL, Humphreys BD. Advantages of single-nucleus over single-cell RNA sequencing of adult kidney: rare cell types and novel cell states revealed in fibrosis. J Am Soc Nephrol 2019;30:23–32

28. Yao L, Romero MJ, Toque HA, Yang G, Caldwell RB, Caldwell RW. The role of RhoA/Rho kinase pathway in endothelial dysfunction. J Cardiovasc Dis Res 2010;1:165–170
29. Godmann M, Kosan C, Behr R. Krüppel-like factor 4 is widely expressed in the mouse male and female reproductive tract and responds as an immediate early gene to activation of the protein kinase A in TM4 Sertoli cells. Reproduction 2010;139:771–782
30. Birsoy K, Chen Z, Friedman J. Transcriptional regulation of adipogenesis by KLF4. Cell Metab 2008;7:339–347
31. Penke LR, Speth JM, Huang SK, Fortier SM, Baas J, Peters-Golden M. KLF4 is a therapeutically tractable brake on fibroblast activation that promotes resolution of pulmonary fibrosis. JCI Insight 2022;7:e160688
32. Hamik A, Lin Z, Kumar A, et al. Kruppel-like factor 4 regulates endothelial inflammation. J Biol Chem 2007;282:13769–13779
33. Atkins GB, Jain MK. Role of Krüppel-like transcription factors in endothelial biology. Circ Res 2007;100:1686–1695
34. Brosius FC 3rd, Alpers CE, Bottinger EP, et al.; Animal Models of Diabetic Complications Consortium. Mouse models of diabetic nephropathy. J Am Soc Nephrol 2009;20:2503–2512
35. Qi H, Casalena G, Shi S, et al. Glomerular endothelial mitochondrial dysfunction is essential and characteristic of diabetic kidney disease susceptibility. Diabetes 2017;66:763–778
36. Fu J, Lee K, Chuang PY, Liu Z, He JC. Glomerular endothelial cell injury and cross talk in diabetic kidney disease. Am J Physiol Renal Physiol 2015;308:F287–F297
37. Daehn IS. Glomerular endothelial cell stress and cross-talk with podocytes in early [corrected] diabetic kidney disease. Front Med (Lausanne) 2018;5:76
38. Chagnac A, Zingerman B, Rozen-Zvi B, Herman-Edelstein M. Consequences of glomerular hyperfiltration: the role of physical forces in the pathogenesis of chronic kidney disease in diabetes and obesity. Nephron 2019;143:38–42
39. Takahashi T, Harris RC. Role of endothelial nitric oxide synthase in diabetic nephropathy: lessons from diabetic eNOS knockout mice. J Diabetes Res 2014;2014:590541